ISSN 1063-7834, Physics of the Solid State, 2012, Vol. 54, No. 4, pp. 748–753. © Pleiades Publishing, Ltd., 2012.
Original Russian Text © R.S. Iskhakov, S.V. Stolyar, L.A. Chekanova, M.V. Chizhik, 2012, published in Fizika Tverdogo Tela, 2012, Vol. 54, No. 4, pp. 704–708.

MAGNETISM

Spin-Wave Resonance in a Multilayer $Co_{1-x}P_x/Co_{1-y}P_y$ Structure as a Method of Detection of the Bragg Gaps in a Spin Wave Spectrum

R. S. Iskhakov[a, *], S. V. Stolyar[a, b], L. A. Chekanova[a], and M. V. Chizhik[b]

[a] *Kirensky Institute of Physics, Siberian Branch of the Russian Academy of Sciences, Akademgorodok 50–38, Krasnoyarsk, 660036 Russia*

* *e-mail: rauf@iph.krasn.ru*

[b] *Siberian Federal University, Svobodnyi pr. 79, Krasnoyarsk, 660041 Russia*

Received July 12, 2011; in final form, September 23, 2011

Abstract—The method of spin-wave resonance has been used to detect in multilayer $(Co_{98}P_2/Co_{95}P_5)_N$ structures a modification of the exchange spin wave spectrum due to the formation of the first, second, and third Brillouin zones in a one-dimensional magnon crystal formed by a periodic modulation of the exchange. The band gaps have been measured for wave vectors $k_b = \pi/(d_1 + d_2)$ and $2k_b$.

DOI: 10.1134/S1063783412040117

1. INTRODUCTION

A spectrum of any waves in periodic structures has a band character. In the spectrum, the bands of allowed and forbidden values of energy ε appear. In the reciprocal space, the Brillouin zones are formed, and the edges are determined by wave vectors $k_b = mq/2$ ($m = 1, 2, 3, ...$), where m is the number of the zone, $q = 2\pi/(d_1 + d_2)$ is the reciprocal lattice vector, and $d_1 + d_2$ is the period of one-dimensional modulation. The $\varepsilon(k)$ function plot has gaps (forbidden bands $\Delta\varepsilon_m$). Among such structures are photon and magnon crystals that are extensively studied at the present time. The theory of wave spectrum in superlattices developed now is oriented for experiments of two classes. In one case, propagating waves are studied using multilayer structures as dielectric mirrors and filters, which is due to appearance of nontransmission bands, and the parameters such as the reflection and transmission coefficients are measured. In the other case, the wave dispersion law $\varepsilon(k)$ is directly studied experimentally. In the experiments, either standing exchange waves (the spin-wave resonance method; see, for example, [1]) or traveling magnetostatic waves (the method of Brillouin scattering [2]) are studied. The wave spectrum of multilayer structures is substantially dependent on superlattice heterogeneities (the interface thickness between layers, layer heterogeneities, and so on [3–5]). To experimentally verify these theoretical conclusions and to illustrate the general physical principles, it is necessary to measure several minibands in a multilayer structure by spectral methods.

In [1, 6], the spin-wave resonance method was used to study the dispersion law of exchange spin waves in $[Ni_{1-x}Fe_x(18\ nm)/Ni_{1-y}Fe_y(18\ nm)]_5$ multilayer films produced by chemical deposition. In this case, the energy gap $\Delta\varepsilon_1$ was detected at $k_5 = 5\pi/L = 5\pi/5(d_1 + d_2) = \pi/(d_1 + d_2) = k_b$, where L is the film thickness. In [1, 6], when analyzing the spin-wave resonance spectrum containing ten spin-wave modes, the concept of the exchange doublet at $n = 5$ was introduced. This doublet is represented by absorption peaks of the energy gap edges of the exchange spin wave spectrum described by the modes $n = 1, 2, 3, 4, 5, 5, 6, 7$, where $k_5 = k_b$. The second Bragg gap at $k = 2k_b$ in $[Ni_{1-x}Fe_x/Ni_{1-y}Fe_y]_5$ structures could not be detected for the following reasons. First, to reliably detect the second Bragg gap in the spin wave spectrum, the total number of recorded spin-wave resonance peaks (trigonometric modes) must be $n \geq 13$ (under the condition that the number of layer pairs in the film is $N = 5$; at $N = 4$, $n \geq 11$). To observe so many resonance peaks, the film thickness must be $L > 350$ nm. Second, in as-prepared multilayer $[Ni_{1-x}Fe_x/Ni_{1-y}Fe_y]_5$ films, the width of the first Bragg gap is $\Delta\varepsilon_1 \approx 1$ kOe. We measured the spin-wave resonance using the microwave-field frequency $f = 9.2$ GHz; because of this, the field scanning is insufficient to detect such a peculiarity of the spin-wave resonance spectrum (in our case, it is 3.0–3.5 kOe).

The aim of this work is to prepare multilayer structures suitable for recording the second Bragg gap in the spin-wave spectrum of multilayer films at $k = 2k_b$, to study the spin-wave resonance spectrum of these films, and to identify the peaks of the spin-wave susceptibility.

2. SAMPLE PREPARATION AND EXPERIMENTAL TECHNIQUE

Standing spin waves in thin ferromagnetic films (thickness L) are excited by a uniform alternating field h. The experimental technique is called the method of spin-wave resonance that is developed well at the present time (e.g., [7, 8]). The absorption peaks recorded are resonances on standing waves with the length $\lambda/2 = L - L/n$, where n is the mode number. The resonance condition is the Kittel relationship

$$H_n = \frac{\omega}{\gamma} + 4\pi M_{\text{eff}} - \frac{2A}{M_S}k^2 \qquad (1)$$

for the case of the orthogonal orientation of an external magnetic field H with respect to the film plane ($H \perp h$). In relationship (1), ω is the fixed frequency of the microwave field, and γ is the gyromagnetic ratio. The magnetization M_{eff} differs from the saturation magnetization M_S by a contribution due to internal stresses in the films and its anisotropy field; k is the wave number of the spin wave ($k = n\pi/L$); A is the constant of exchange interaction ($A = \alpha M_S^2/2$, where α is the exchange parameter). As the spins are completely pinned at the film surface (nodes of the standing waves), the microwave contains only odd modes (n = 1, 3, 5, ...). When the pinning is incomplete, even modes also can appear. In addition, depending on the pinning sign described by the surface anisotropy K_S, the spectrum can contain surface spin waves at $K_S < 0$. The spin-wave resonance is used now above all in measurements of the exchange constant, among them, in films of heterogeneous ferromagnets such as amorphous and nanocrystalline alloys. The effective spin-wave stiffness of films of heterogeneous alloys is calculated by the formula

$$\eta = \frac{2A}{M_S}\left(\frac{\pi}{L}\right)^2 = \frac{H_1 - H_i}{n_i^2 - 1}. \qquad (2)$$

The multilayer Co–P-based films under study were prepared by chemical deposition. At the external surface of thus-prepared ferromagnetic (metal/air interface) films, the surface easy-plane-type anisotropy $K_S \approx 1$ erg/cm^2 forms naturally. The magnitude and sign of the surface pinning of the magnetization vector in near-substrate part of the film were formed by deposition of additional ferromagnetic layer exchange-bounded with the main part of the film [9]. It was shown in [9] that the deposition on a ferromagnetic film of additional exchange-bounded ferromagnetic layer (with lesser thickness) with the magnetization lesser than that of the film leads to the formation of the anisotropy of easy-axis type ($K_S > 0$). On the other hand, the deposition on a ferromagnetic film of additional ferromagnetic layer exchange-bounded with the film with the magnetization higher than that of the film leads to the formation of the surface anisotropy of the easy-plane type ($K_S < 0$). The magnitude of the surface anisotropy is determined by the thickness of the additional layer and the magnitude of the exchange interaction between the layers.

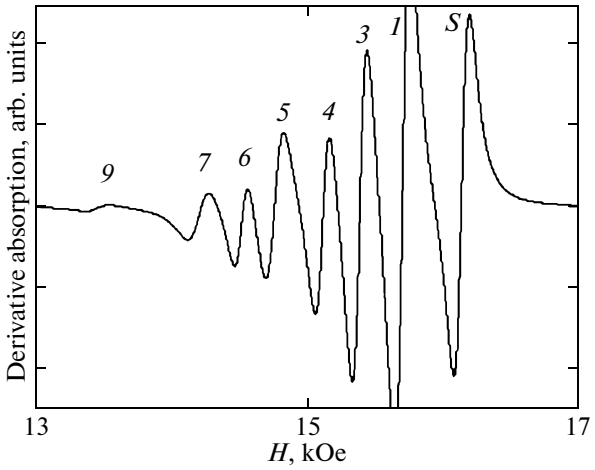

Fig. 1. Spin-wave resonance spectrum of a single-layer 300-nm-thick $Co_{95}P_5$ film.

The alloys used for preparing one-layer and multilayer films were characterized by the parameters as follows [10]: fcc Co, composition $Co_{95}P_5$, the field of local anisotropy $H_a = 2$ kOe, $M_S = 890$ G, $\alpha = 2.4 \times 10^{-12}$ cm^2; hcp Co, composition $Co_{98}P_2$, $H_a = 7$ kOe, $M_S = 950$ G, $\alpha = 1.3 \times 10^{-12}$ cm^2. The thicknesses of individual layers in multilayer structures differed insignificantly. The number of layer pairs was $N = 4, 5, 7$. The spectra of ferromagnetic resonance and spin-wave resonance were measured on an EPA-2M standard spectrometer at a frequency of 9.2 GHz at room temperature. The single-layer 300-nm-thick $Co_{98}P_2$ films demonstrate the only absorption with the ferromagnetic resonance line width $\Delta H = 700$ Oe.

3. RESULTS AND DISCUSSION

Figure 1 shows the spin-wave resonance spectrum of the single-layer $Co_{95}P_5$ film with the thickness L = 300 nm. The spin-wave resonance spectrum contains eight peaks, which allows us to perform a complete analysis of the spectrum. It is seen that the spectrum of this film has the absorption whose resonance field higher than the field of the most intense absorption. The surface peak is due to the surface vibration of the magnetization. The latter means that the wave vectors k of the standing spin waves are determined using equations [7, 8] obtained from the exchange boundary conditions at arbitrary parameters of pinning of the

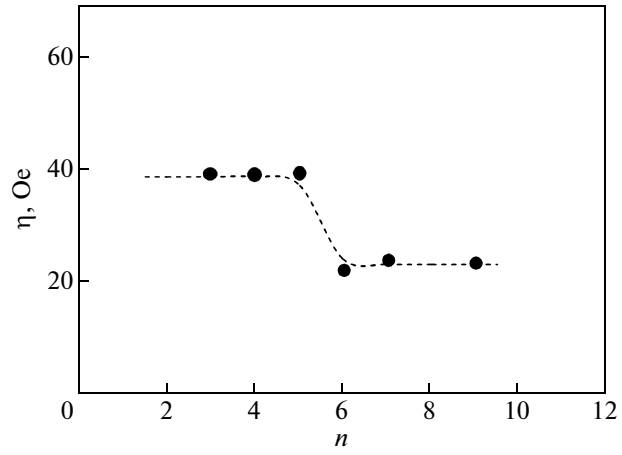

Fig. 2. Dependence of the effective spin-wave stiffness η on the mode number in the spin-wave resonance spectrum of the 300-nm-thick $Co_{95}P_5$ film. The wave vector of the standing spin wave is $k_n = n(\pi/L)$.

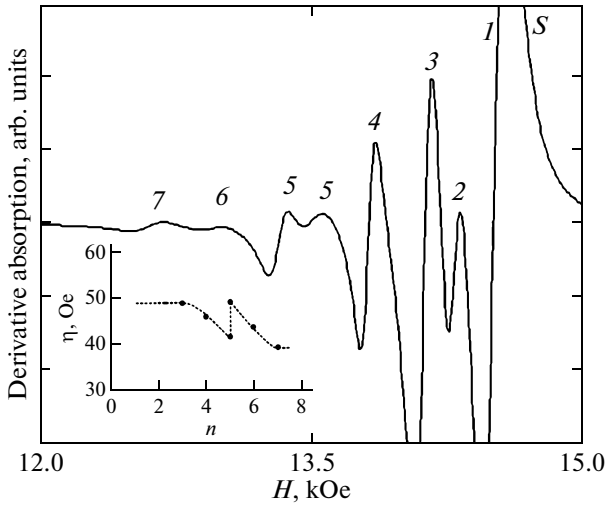

Fig. 3. Spin-wave resonance spectrum of the multilayer $[Co_{98}P_2(30\ nm)/Co_{95}P_5(20\ nm)]_5$ film. The inset shows the dependence of the effective spin-wave stiffness η on the mode number in the spin-wave resonance spectrum of this film. The wave vector of the standing spin wave is $k_n = n(\pi/L)$.

magnetization at the bottom and top surfaces of the film d_1^S and d_2^S:

$$\tan(kL) = \frac{(d_1^S + d_2^S)k}{k^2 - d_1^S d_2^S}, \quad (3)$$

when k is real, and

$$\tanh(k_S L) = \frac{-(d_1^S + d_2^S)k_S}{k_S^2 + d_1^S d_2^S}, \quad (4)$$

when $k = ik_S$ is imaginary.

Here, the pinning parameter is $d_i^S = K_{iS}/A$. The quantity A/K_S is indicative of the fictive displacement of a standing wave node from the film surfaces. The existence of the surface mode labeled S in Fig. 1 is indicative of realization of the easy-plane-type anisotropy at either external or near-substrate surfaces of the film. Recording the field coordinate of the S mode allows direct measurement of the value of K_S: $|K_S| = 6.2\ erg/cm^2$. For volume modes, in the case of strong pinning ($A/K_S L \longrightarrow 0$), Eq. (3) has the Kittel solution $kL = n\pi$ with excitation only of odd n. In the case $|A/K_S L| < 1$, we obtain the solution

$$kL = n\pi(1 - A/K_S L) = n\beta, \quad (5)$$

where $n = 1, 2, 3, ...$, i.e., both odd modes (symmetric with respect to the film center) and even modes (antisymmetric with respect to the film center) are excited in the spectrum. Because of their antisymmetricity, the even modes have lower intensity as compared to the intensities of surrounding odd modes. Actually, for $n = 4$: $I_4 \ll I_3$ and $I_4 < I_5$; for $n = 6$: $I_6 \ll I_5$ and $I_6 < I_7$ (the even peaks with $n = 2$ and 8 are not manifested in the spectrum). For the single-layer $Co_{95}P_5$ film with the thickness $L = 300$ nm, parameter $\beta \approx 3.124$. Since the spin-wave mode width (~200 Oe) exceeds the resonance field shift by an order in magnitude, wave vectors k_n can be found using the Kittel solution.

The identification of numbers of spin-wave modes shown in Fig. 1, allows one, using Eq. (2), to find, for the nanocrystalline ferromagnet $Co_{95}P_5$, the constant of inhomogeneous exchange interaction that characterizes additional exchange energy appeared in the spin wave. The values of η_i calculated by Eq. (2) are given in Fig. 2. It is seen that the exchange spin waves with the wave length $\lambda/2 = L - L/5$ are characterized by higher value of $\tilde{\eta}$, and short spin waves with $\lambda/2 = L/6 - L/9$ are characterized by lower value of $\tilde{\eta}$. This effect is due to the influence of correlated heterogeneities on the spin-wave spectrum. The effect was predicted theoretically in [11] and was repeatedly confirmed in subsequent theoretical studies (e.g., [12, 13]). A main result of the works cited is that the dispersion (and damping) laws must be modified in the vicinity of the correlation wave number ($1/r_c$), and the modifications are different for the heterogeneities of various physical parameters. Based on this theory, the experimental method of correlation spin-wave spectroscopy was developed, and this method was used to measure the correlation radii of the heterogeneities for many amorphous and nanocrystalline alloys (e.g., review [14] and recent works [15, 16]). The $\tilde{\eta}(k)$ dependence shown in Fig. 2 is due to heterogeneities of the exchange parameter, and the measurement of the critical spin-wave length λ_c ($\lambda/2 = L/6 = 50$ nm) permits one to determine the spatial scale of this het-

erogeneity ($2r_c \approx 50$ nm) of the nanocrystalline $Co_{95}P_5$ alloy.

Figure 3 shows the spin-wave resonance spectrum of the multilayer $[Co_{98}P_2(30\ nm)/Co_{95}P_5(20\ nm)]_5$ film. Here, the identification of recorded resonance absorption is given as well. It is seen that the first resonance absorption is the superposition of two peaks: surface vibration labeled S in Fig. 3 and the absorption $n = 1$ due to the first trigonometric mode. The latter indicates on a possibility of appearance of even modes in the spectrum, i.e., the necessary identification is $n = 1, 2, 3, 4, 5$. For the multilayer $[Co_{98}P_2(30\ nm)/Co_{95}P_5(20\ nm)]_5$ film with $|K_S| = 1.2$ erg/cm^2, the parameter $\beta = 3.04$. Because of this, the wave vectors k_n can be found using the Kittel solution (shift of the resonance fields of the spin-wave modes is smaller than their line widths).

Of specific interest is the fifth mode, since it is characterized by the wave vector $k_5 = 5\pi/L = \pi/5(d_1 + d_2) = \pi/(d_1 + d_2) = k_b$, i.e., this peak exists at the low-energy edge of the energy gap of the spin-wave spectrum. Then, the identification n of low-field peaks of the spin-wave resonance of this film must be continued as follows: $n = 5, 6, 7$ as demonstrated by the intensities of the modes observed. Thus, as in [1, 6], we introduce the exchange doublet at $n = 5$ that is the absorption peaks of the forbidden band edges of the exchange spin wave spectrum described by the modes $n = 1, 2, 3, 4, 5, 5, 6, 7$, where $k_5 = k_b$. The modes $n = 1, 2, 3, 4, 5$ characterize the first Brillouin zone of a magnon crystal, and the modes $n = 5, 6, 7$ characterize the second Brillouin zone (inset to Fig. 3). The forbidden band width is measured in the field coordinates as the difference of magnitudes of constant fields characterizing the fifth modes; for the $[Co_{98}P_2(30\ nm)/Co_{95}P_5(20\ nm)]_5$ film, it is 180 Oe. This width of the forbidden gap is substantially smaller than the gap width observed in [1, 6] when the spin-wave resonance spectrum of the multilayer $[Ni_{65}Fe_{35}(18\ nm)/Ni_{60}Fe_{40}(18\ nm)]_5$ film was studied. The reason of the differences is due to different modulating magnetic parameters. In the multilayer $[Ni_{65}Fe_{35}(18\ nm)/Ni_{60}Fe_{40}(18\ nm)]_5$ structure, the chemical compositions of the used layers were chosen so that the main modulating parameter was the saturation magnetization. The main modulating parameter of multilayer structures based on Co–P alloys under study is the magnitude of the exchange interaction (and also the magnitude of the field of local anisotropy).

Figure 4 shows the spin-wave resonance spectrum of the multilayer $[Co_{98}P_2(40\ nm)/Co_{95}P_5(50\ nm)]_4$ structure. This spectrum contains 13 peaks, which allows the complete analysis of the noted spectra.

The spectrum of this film has two peaks whose resonance fields are higher than the field of the most intense maximum. The peaks correspond to the excitation of two surface modes ($n = 0$) labeled S_1 and S_2

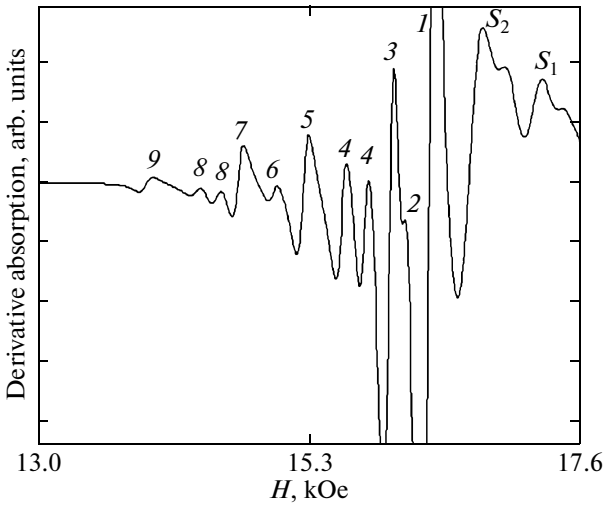

Fig. 4. Spin-wave resonance spectrum of the multilayer $[Co_{98}P_2(40\ nm)/Co_{95}P_5(50\ nm)]_4$ film.

in Fig. 4. The peaks demonstrate the realization of exchange boundary conditions with the surface easy-plane anisotropy at the external and near-substrate surfaces of this multilayer film. The latter shows that the spectral curve contains both odd modes (high intensity) and even modes (low intensity), i.e., the identification of spin-wave modes is $n = 1, 2, 3, \ldots$.

The multilayer $[Co_{98}P_2(40\ nm)/Co_{95}P_5(50\ nm)]_4$ film with the constants of surface anisotropies $|K_{S1}| = 15$ erg/cm^2 and $|K_{S2}| = 5.9$ erg/cm^2 has the parameter $\beta \approx 3.13$. Because of this, the wave vectors also can be found using the Kittel solution (the error does not exceed 1%).

Of particular interest are the doublets of the fourth and eighth modes, since they are characterized by the wave vectors $k_4 = k_b$ and $k_8 = 2k_b$, respectively.

Figure 5a presents the values of $\tilde{\eta}_i$ calculated using Eq. (2). It is seen that the exchange parameter $\tilde{\eta}_i$ of the standing spin waves that manifest themselves in modes 1, 2, 3, 5, 6, 7, 9 is described by the $\tilde{\eta}(k)$ dependence that is due to the inhomogeneities of the exchange parameter (the dashed curve in Fig. 5a is similar to the $\eta(k)$ curve in Fig. 2). The latter allows introduction of the critical spin wave length $\lambda_c = \lambda_6$: spin waves with $\lambda > \lambda_c$ are characterized by higher value of $\tilde{\eta}_i$, and spin waves with $\lambda < \lambda_c$ have lower value of $\tilde{\eta}_i$ ($\lambda_c/2 = 2r_c = 60$ nm). Doublets of the fourth mode of the spectral curve manifest themselves by two ordinates $\tilde{\eta}_i^{(I, II)}$ for the spin wave $\lambda_b/2 = d_1 + d_2 = 90$ nm, and doublets of the eighth mode manifest themselves by two ordinates $\tilde{\eta}_8^{(I, II)}$ for the spin wave with $\lambda_b/2 = (d_1 + d_2)/2 = 45$ nm. The waves are

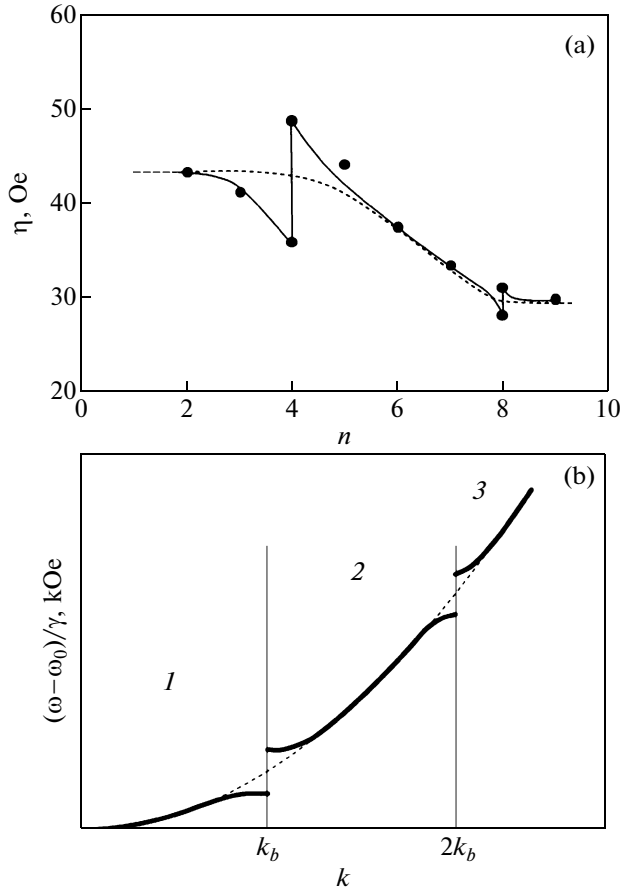

Fig. 5. (a) Dependence of the effective spin-wave stiffness η on the mode number in the spin-wave resonance spectrum of the multilayer $[Co_{98}P_2(40\ nm)/Co_{95}P_5(50\ nm)]_4$ film. The wave vector of the standing spin wave is $k_n = n(\pi/L)$. (b) Dispersion law of spin waves in a multilayer structure (schematically).

described by the wave vectors $k_4 = k_b$ and $k_8 = 2k_b$, i.e., the Brillouin zone boundaries of a magnon crystal (Fig. 5b). Figure 5b schematically shows the dispersion law of exchange spin waves in the multilayer film. The dashed line describes the dispersion law in the homogeneous ferromagnetic film.

In the spin-wave resonance spectrum of the multilayer $[Co_{98}P_2/Co_{95}P_5]_4$ film (Fig. 4), modes $n = 1, 2, 3, 4$ characterize the first Brillouin zone of the magnon crystal; modes 4, 5, 6, 7, 8 characterize the second Brillouin zone, and modes 8 and 9 characterize the third Brillouin zone. The intensities of the observed spin-wave modes satisfy the above-stated rules. The forbidden gap width is measured in the field coordinates as the difference between the fields characterizing the doublets of the spin-wave modes. For this multilayer structure, the forbidden gap widths $\Delta\varepsilon_1$ and $\Delta\varepsilon_2$ are 200 and 180 Oe, respectively. The results presented in Fig. 5 indicate that the observed modification of the $\eta(k)$ dependence as a result of joint action of two factors: the isotropic fluctuations of the exchange parameter and the one-dimensional periodic modulation of the exchange in the multilayer $[Co_{98}P_2/Co_{95}P_5]_N$ system.

4. CONCLUSIONS

Thus, using the method of spin-wave resonance for exchange spin wave, we detected the modification of the spin-wave spectrum due to the formation of the first, second, and third Brillouin zones in the one-dimensional magnon crystals prepared as multilayer ferromagnet/ferromagnet structures. The forbidden gap widths measured in the field coordinates in the exchange spin-wave spectrum of the multilayer $[Co_{98}P_2/Co_{95}P_5]_N$ film $\Delta\varepsilon_1 = 200$ Oe and $\Delta\varepsilon_2 = 180$ Oe are smaller by a factor of five–seven than similar characteristics of the multilayer $[NiFe/NiFe]_N$ films.

ACKNOWLEDGMENTS

This study was supported by the Ministry of Education and Science of the Russian Federation within the framework of the Analytic Department Targeted Program "Development of the Scientific Potential of the Higher School (2011)" and Russian Federal Targeted Program "Scientific and Scientific–Pedagogical Human Resources for the Innovative Russia in 2009–2013."

REFERENCES

1. R. S. Iskhakov, L. A. Chekanova, and S. V. Stolyar, in *Proceedings of the 12th International Meeting "Ordering in Minerals and Alloys,"* Rostov-on-Don, Russia, September 10–16, 2009 (Southern Federal University, Rostov-on-Don, 2009), Vol. 1, p. 214.
2. Z. K. Wang, V. L. Zhang, H. S. Lim, S. C. Ng, M. H. Kuok, S. Jain, and A. O. Adeyeyev, Appl. Phys. Lett. **94**, 083112 (2009).
3. V. A. Ignatchenko, Yu. I. Mankov, and A. A. Maradudin, Phys. Rev. B: Condens. Matter **62**, 2181 (2000).
4. V. V. Kruglyak and A. N. Kuchko, Physica B (Amsterdam) **339**, 130 (2003).
5. V. A. Ignatchenko, Yu. I. Mankov, and D. S. Tsikalov, JETP **107** (4), 603 (2008).
6. R. S. Iskhakov, S. V. Stolyar, L. A. Chekanova, and M. V. Chizhik, Solid State Phenom. **168–169**, 73 (2011).
7. N. M. Salanskii and M. Sh. Erukhimov, *Physical Properties and Applications of Magnetic Films* (Nauka, Novosibirsk, 1975) [in Russian].
8. A. G. Gurevich, *Magnetic Resonance in Ferrites and Antiferromagnets* (Nauka, Moscow, 1973) [in Russian].

9. Yu. A. Korchagin, R. G. Khlebopros, and N. S. Chistyakov, Sov. Phys. Solid State **14** (7), 1826 (1972); Yu. A. Korchagin, R. G. Khlebopros, and N. S. Chistyakov, Fiz. Met. Metalloved. **34**, 1303 (1972).
10. R. S. Iskhakov, G. V. Popov, and M. M. Karpenko, Fiz. Met. Metalloved. **56**, 85 (1983).
11. V. A. Ignatchenko and R. S. Iskhakov, Sov. Phys. JETP **45** (3), 526 (1977).
12. M. V. Medvedev and M. V. Sadovskii, Sov. Phys. Solid State **23** (7), 1135 (1981).
13. K. Handrich and R. Ottking, Phys. Status Solidi B **216**, 1073 (1999).
14. V. A. Ignatchenko and R. S. Iskhakov, in *Magnetic Properties of the Crystalline and Amorphous Mediums* Ed. by V. A. Ignatchenko (Nauka, Novosibirsk, 1989), p. 128 [in Russian].
15. R. S. Iskhakov, S. V. Stolyar, L. A. Chekanova, and V. S. Zhigalov, Phys. Solid State **43** (6), 1108 (2001).
16. R. S. Iskhakov, D. E. Prokof'ev, L. A. Chekanova, and V. S. Zhigalov, Tech. Phys. Lett. **27** (4), 344 (2001).

Translated by Yu. Ryzhkov